Photocatalysis of Perfluorinated Oligo(*p*-Phenylene)s

Katsuya MARUO, Yuji WADA, and Shozo YANAGIDA*
Chemical Process Engineering, Faculty of Engineering, Osaka University,
Suita, Osaka 565
(Received May 18, 1992)

Perfluorination of oligo(*p*-phenylene)s (OPP-*n*), biphenyl(OPP-2) to *p*-quaterphenyl (OPP-4), induces various changes in the spectral and physical characteristics of OPP-*n*; a hypsochromic shift of their absorption spectra, a decrease in their fluorescence quantum yields, an increase in their fluorescence lifetimes, and a positive shift of their oxidation potentials. The resulting perfluorinated oligo(*p*-phenylene)s (F-OPP-*n*, *n*=3 and 4) shows photocatalytic activities for the photoreduction of water and for the photooxidation of benzene to phenol. Irradiation of an aqueous methanol solution of F-OPP-3 with triethylamine as an electron donor, and noble metal colloid as an electron mediator at λ>290 nm, leads to H_2 evolution, although photodefluorination through F-OPP-3$^{-\cdot}$ inevitably occurs to an appreciable extent. A similar irradiation of an aqueous acetonitrile solution with O_2 and benzene induces the oxidation of benzene and water, yielding almost equal quantities of phenol and H_2O_2 without any accompanying degradation of F-OPP-3.

Perfluorinated aliphatic compounds show high stabilities against heat, oxidation, and chemical reagents owing to a strong well-packed sp^3–carbon–fluorine bond attributable to the largest electronegativity and the smallest van der Waals radius of the fluorine atom. With regard to perfluorinated aromatic compounds, however, only limited numbers of studies concerning their properties and reactions have been reported, i.e., photo-induced valence-bond isomerization of perfluorinated 6-membered aromatic compounds,[1] thermal stability,[2a] spectral characteristics[3,4] of some fluorinated oligo(*p*-phenylene)s, nonbonded interactions of polyfluorinated aromatic compounds,[5] and photoinduced defluorination of polyfluorobenzene.[6]

On the other hand, we recently clarified that linear aromatic compounds, such as oligo(*p*-phenylene)s (OPP-*n*), i.e., *p*-terphenyl (OPP-3) to *p*-sexiphenyl (OPP-6), and poly(pyridine-2,5-diyl), show homogeneous or heterogeneous photocatalysis for the photoreduction of water, ketones, and alkenes in the presence of triethylamine (TEA) as a sacrificial electron donor.[7,8] The important findings concerning their catalysis are that anion radicals formed by a reductive quenching of excited linear aromatics serve as crucial intermediates for a subsequent electron transfer to electron-accepting substrates, and that the suppression of degradative side reactions, such as an electrophilic attack of protons on the anion radicals, is a requisite for their continued photocatalysis. The quinonoid-like structures of the anion radicals suggest a delocalization of the spin density of the radical anions, causing a suppression of the attack of electrophiles, such as the proton. Further, when noble metal colloids are present in the systems, they mediate a smooth electron transfer from the anion radicals to protons, leading to an efficient photocatalytic H_2 evolution in the presence of water.

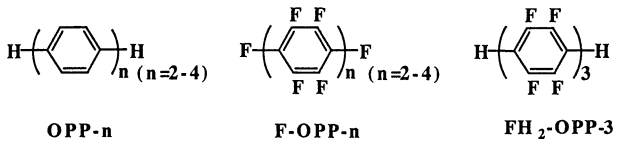

OPP-n F-OPP-n FH_2-OPP-3

Scheme 1.

These findings and the very limited photochemical knowledge concerning fluorinated aromatics prompted us to examine the photophysical and photochemical properties of perfluorinated oligo(*p*-phenylene)s, F-OPP-*n* (*n*=2—4). The objective of this study was to characterize their spectral and photochemical properties in comparison with those of nonfluorinated oligo(*p*-phenylene)s, OPP-*n*, and to clarify their photocatalytic activities and perfluorination effect on the characteristics of the photoformed intermediary species in terms of their computer(MOPAC)-simulated structures. The structure and abbreviations of the oligo (*p*-phenylene) derivatives are shown in Scheme 1.

Results and Discussion

Spectral and Physical Characteristics of Perfluorinated Oligo(*p*-Phenylene)s (F-OPP-*n*). The absorption spectra of F-OPP-*n* (*n*=2—4) were measured in a THF solution and compared with those of the corresponding OPP-*n* (Fig. 1). The onset of the absorption spectra of the F-OPP-*n* series arises at shorter wavelengths than those of OPP-*n*; the shift caused by an increase in the number of perfluorophenylene rings is smaller than that of the nonfluorinated OPP-*n* series. These facts suggest that F-OPP-*n* should comprise noncoplanar and poorly conjugated perfluorinated phenylene rings, even when the number of perfluorinated phenylene rings increases up to 4.

Figure 2 shows the emission spectra of F-OPP-*n* and OPP-*n*, where the intensity is normalized. It is interesting to note that the emission spectra of the F-OPP-*n* series do not show any vibrational structures, but that those of the OPP-*n* series show remarkable vibrational structures. The energy gaps (E_g) were determined by considering the spectral characteristics in a THF solu-

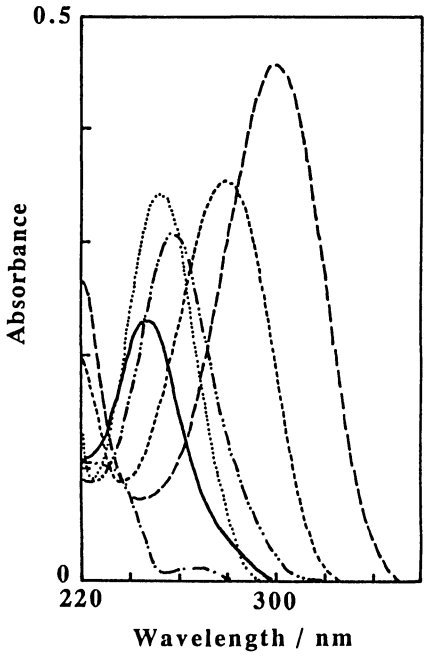

Fig. 1. Absorption spectra of F-OPP-*n* and OPP-*n* in THF solution: (—·—) F-OPP-2; (——) F-OPP-3; (—- - -—) F-OPP-4; (------) OPP-2; (– – –) OPP-3; (— —) OPP-4. These concentrations are 1.0×10^{-5} mol dm^{-3}.

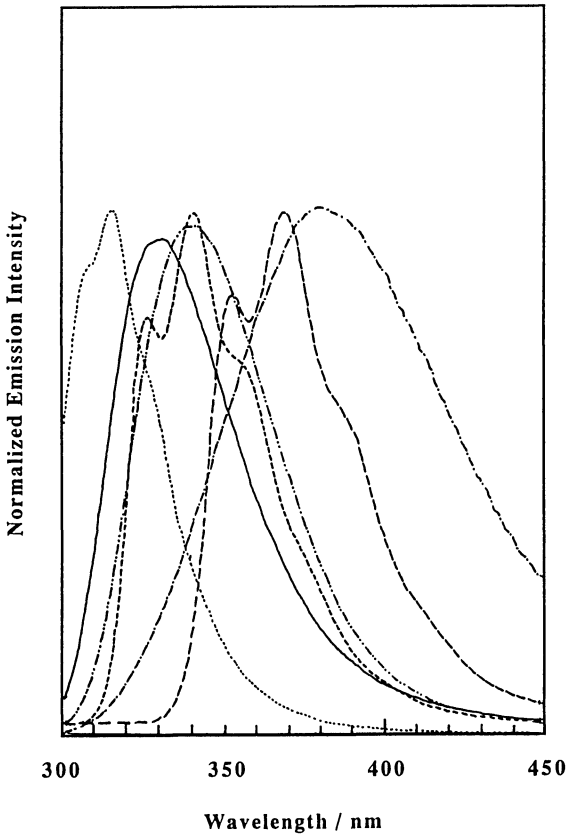

Fig. 2. Emission spectra of F-OPP-*n* and OPP-*n* in THF solution: (—·—) F-OPP-2; (——) F-OPP-3; (—- - -—) F-OPP-4; (·····) OPP-2; (------) OPP-3; (– – –) OPP-4. These emission intensities are normalized.

tion. The spectral properties, including the emission lifetimes and quantum yields of their maximum emission in a THF solution, as well as the solubilities, are summarized along with those of OPP-*n* in Table 1. It is apparent that the perfluorination of OPP-*n* affects their spectral characteristics. There is a large shift in the positions of the absorption band and the excitation spectra toward shorter wavelengths (hypsochromic shift), which accompanies a small bathochromic shift with an increase in the number of the phenylene rings, compared with that of OPP-*n*. The hypsochromic shift is true for the emission spectra, except for the emission of F-OPP-2. It is worth noting that the lifetimes of the emission of F-OPP-*n* increase while their quantum yields decrease. The perfluorination slightly improves the solubility for OPP-3 and OPP-4 in methanol, probably due to a weakened intermolecular force induced by perfluorination.

For the purpose of making a quantitative evaluation of the energy structures of F-OPP-*n* and OPP-*n*, their thermodynamic oxidation potentials were measured by voltammetric techniques (Table 2). Although both derivatives exhibited irreversible oxidation waves, making the accuracy of E_{OX} doubtful, F-OPP-3 in acetonitrile on a Pt electrode showed a broad voltammetric oxidation peak at 2.07 V vs. SCE, and OPP-3 showed it at 1.70 V vs. SCE. By taking account of the E_g values in a THF solution, the energy structures of F-OPP-*n*

Table 1. Physical and Spectral Characteristic Data of F-OPP-*n* and OPP-*n* in Solution[a)]

p-Phenylene	λ_{max} (log ε)[b)]/nm	E_x[c)]/nm	E_m[d)]/nm	E_g[e)]/eV	τ_{EM}[f)]/ns	Φ_{EM}[g)]	Solubility[h)]
F-OPP-2	220(4.00)	235	380	4.2	—	0.04—0.06	215
F-OPP-3	246(4.35)	245	331	4.2	23	0.1	1.87
F-OPP-4	255(4.48)	254	338	4.2	24	0.1	0.18
OPP-2	250(4.53)	253	316	4.3	15	0.2	391
OPP-3	278(4.55)	287	341	3.9	0.8	1.0	1.22[i)]
OPP-4	297(4.66)	309	367	3.6	0.7	0.8	0.02[i)]

a) Measured in THF: [*p*-Phenylene]=1.0×10^{-5} mol dm^{-3}. b) λ_{max} is absorption maximum wavelength and ε is extinction coefficient. c) Excitation maximum wavelength. d) Emission maximum wavelength. e) Energy gap estimated from spectral data. f) Observed emission lifetime. g) Emission quantum yield. h) Measured in MeOH (mmol dm^{-3}). i) See Ref. 7b.

Table 2. Electronic Structure of F-OPP-*n* and OPP-*n*

p-Phenylene	E_g[a)]/eV	E_{Ox}[b)]/V	E_{Red}[c)]/V
F-OPP-2	4.4	—	—
F-OPP-3	4.2	2.07	−2.13
F-OPP-4	4.2	—	—
OPP-2	4.3 (4.49)[d)]	1.99 (1.91)[d)]	−2.31 (−2.58)[d)]
OPP-3	3.9	1.70	−2.20 (−2.40)[e)]
OPP-4	3.6	1.56	−2.04 (−2.28)[e)]

a) Measured in THF. See Table 1. b) Oxidation peak potentials were measured in acetonitrile vs. SCE. c) Reduction potentials were calculated from $E_{Red}=E_{Ox}-E_g$. d) The oxidation potential was measured in DMF vs. SCE and the reduction potential was measured in acetonitrile vs. SCE. See Ref. 9a. e) The reduction potentials were measured in dimethylamine vs. Ag/AgCl. See Ref. 9b.

(n=3,4) were determined, and are summarized along with those of OPP-*n* in Table 2.[9)]

Photochemical Properties of F-OPP-*n*. A recent study concerning the UV (λ=254 nm)-induced photolysis of pentafluorobenzene[6)] revealed that photodefluorination proceeds through excimer formation in acetonitrile or pentane, as well as through exciplex formation with electron donors, such as triethylamine (TEA).[6)] By taking these results into account, we could investigate the photolysis of F-OPP-3 in some solvents.

As shown in Fig. 3, F-OPP-3 underwent rapid photodegradation under λ>290 nm irradiation in a solvent such as methanol or THF. It is interesting to note that UV-irradiated F-OPP-3 is rather stable in benzene as well as in acetonitrile. The oxidation potentials of solvents (e.g., methanol 3.09, benzene 2.40 V vs. SCE.)[10)] are too large to attribute the photodegradation to an electron transfer from the solvent to the photoexcited F-OPP-3, when compared with the estimated oxidation potential of F-OPP-3, i.e., 2.07 V vs. SCE (Table 2).

The photodegradation was found to be quenched by oxygen. Further, as shown in Fig. 3, the photodegradation of F-OPP-3 also occurred in THF under λ=366 nm irradiation only in the presence of benzophenone, a sensitizer of λ=366 nm light.

In addition, photodegradation in THF depends on the concentration of F-OPP-3 (within the concentration range of 0.0002—0.001 mol dm^{-3}.), suggesting participation of the excimer from F-OPP-3. Figure 4 shows a double-reciprocal plot of the quantum yield of the consumption of F-OPP-3 vs. the concentration of F-OPP-3; it provides a clear linear plot with the intercept (i), slope (s), and intercept-to-slope ratio (i/s) (i=3.47, s=0.00313 mol dm^{-3}, and i/s=1108 dm^3 mol^{-1}, respectively). Assuming the singlet excimer mechanism for the degradation of F-OPP-3, the rate constant for the formation of the excimer (k_r), which can be calculated by dividing i/s by the lifetime of singlet F-OPP-3 (termed τ=20 ns in Table 1), exceeds 10^{10} dm^3 mol^{-1} s^{-1}. The k_r value may be too large to consider the formation of the singlet

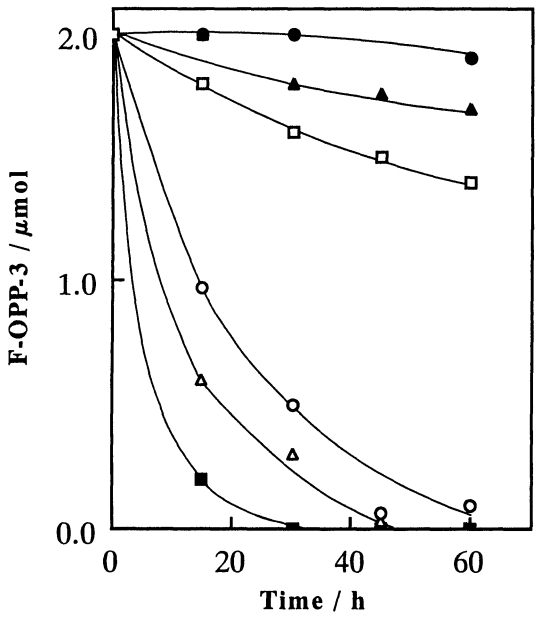

Fig. 3. Photolysis of F-OPP-3 in benzene (●), acetonitrile (▲), tetrahydrofuran (■), methanol (○), cyclohexane (△) under irradiation at >290-nm, and tetrahydrofuran (□) in the presence of benzophenone under >366-nm irradiation.

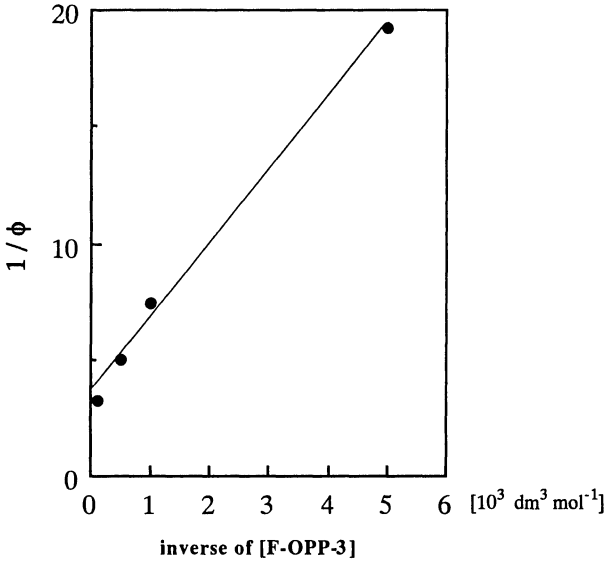

Fig. 4. Double reciprocal plot of the quantum yields for the photodefluorination of F-OPP-3 ($1/\phi$) vs. the concentration of F-OPP-3.

excimer. With these observations, it was concluded that the photodegradation of F-OPP-3 should proceed through a triplet excimer, as was confirmed regarding the photolysis of pentafluorobenzene.[6,11,12)]

As another source of evidence supporting excimer formation, i.e., the formation of F-OPP-3$^{-\cdot}$ and F-OPP-3$^{+\cdot}$ in a solvent cage, 2,2′,2″,3,3′,3″,5,5′,5″,6,6′,6″-dodecafluoro-*p*-terphenyl (FH_2-OPP-3) was isolated and confirmed to be a defluorinated product from the

former intermediate.[6b] The benzophenone-sensitized photodegradation of F-OPP-3 also gave FH_2-OPP-3, supporting the formation of the excimer via the triplet state. Further, a methoxylated product ($C_{18}F_{13}OCH_3$) was detected by GC-Mass analysis as a substitution product from F-OPP-3$^{+\cdot}$.[12b]

It was reported that the photoexcited pentafluorobenzene undergoes defluorination in the presence of TEA through exciplex formation.[6b] Also, in the case of F-OPP-3, defluorination was found in the presence of TEA. UV experiments provided no evidence for a ground-state charge-transfer complex under the reaction conditions. It was speculated that the presence of TEA led to the photodegradation of F-OPP-3 through an effective formation of F-OPP-3$^{-\cdot}$ from the exciplex.

F-OPP-*n*-Catalyzed H_2 Evolution in the Presence of Noble Metal Colloids. Taking account of the above-mentioned spectral and energetic characteristics, as well as the role of colloidal ruthenium metal (Ru^0) as an electron mediator in the OPP-*n*-catalyzed H_2 evolution,[7] F-OPP-3-catalyzed photoreduction of water was attempted in the presence of either Ru^0, as an electron mediator,[13] or ruthenium chloride ($RuCl_3$), as a source of Ru^0. Aqueous methanolic suspensions of F-OPP-3 and Ru^0 or $RuCl_3$ were irradiated with TEA as an electron donor under $\lambda>290$ nm light. As shown in Fig. 5, H_2 evolution was observed in both cases. F-OPP-3 showed little activity in the absence of either Ru^0 or $RuCl_3$. The H_2 evolution in the presence of Ru^0 was initiated at the beginning of irradiation. On the other hand, an induction period was observed when $RuCl_3$ was used instead of Ru^0. During the induction period, $RuCl_3$ should be photoreduced through an electron transfer from F-OPP-3$^{-\cdot}$, giving Ru^0. It was therefore concluded that Ru^0 should mediate an electron transfer from F-OPP-3$^{-\cdot}$ to a proton and/or water, as was observed for the OPP-*n* system.[7]

Figure 6 shows the effect of noble metal colloids on F-OPP-3-catalyzed H_2 evolution. As sources of metal colloids, metal halides were employed in the photoreaction, as well as in the case of Ru^0. Interestingly, H_2 evolution depends on noble metal colloids, and colloidal Rh^0 gave the best co-catalytic activity, while Pd^0 colloid showed poor activity.

Photolysis in D_2O with a F-OPP-3/$RhCl_3$ system gave a mixture of D_2, DH, and H_2 in a 76:20:3 ratio. This fact suggests that the major source of H_2 should be water.[7]

In the F-OPP-3/$RuCl_3$ system, diethylamine (DEA) and a small amount of ethanol were formed in addition to H_2 and Ru^0, as well as in the photocatalysis of OPP-*n*.[7] DEA should be formed from a two-electron oxidation of TEA, i.e., hydrolysis of $Et_2NC^+HCH_3$, whereas ethanol arises from a reduction of the resulting acetaldehyde. The photoreductive H_2 evolution with F-OPP-3, F-OPP-4, and nonfluorinated oligo(*p*-phenylene)s (OPP-*n*, *n*=3,4) was examined and compared under comparable conditions using $RuCl_3$ as the source of an electron mediator (Fig. 7). After an induction period, which implies the formation of colloidal Ru^0, the rate of the F-OPP-3-catalyzed H_2 evolution was comparable to that of the OPP-3 system; that of the F-OPP-4 system, however, gave superior activity with only a short induction period, compared with that of the OPP-4 system.

Table 3 summarizes the formation of H_2, DEA, and ethanol. F-OPP-2 showed only negligible activity, as

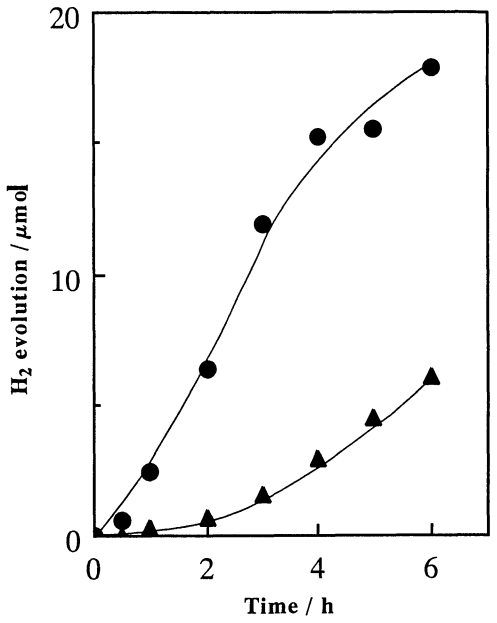

Fig. 5. Water-photoreductive H_2 evolution catalyzed by F-OPP-3 in the presence of prepared Ru colloid (●) and $RuCl_3$ (▲).

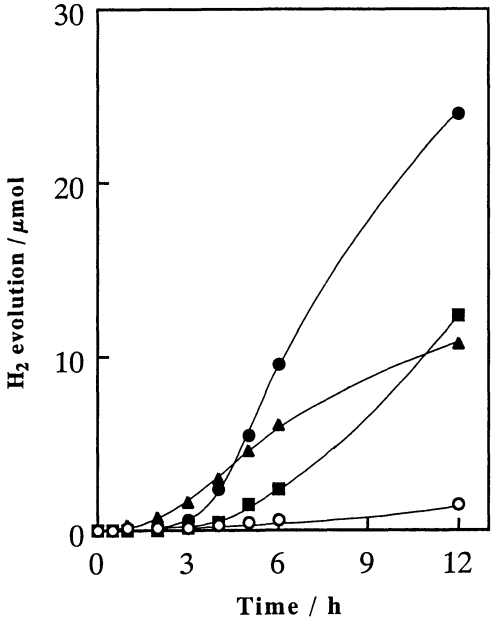

Fig. 6. Effect of noble metals on the formation of H_2 photocatalyzed by F-OPP-3: (●) $RhCl_3$; (▲) $RuCl_3$; (■) H_2PtCl_6; (○) $PdCl_2$.

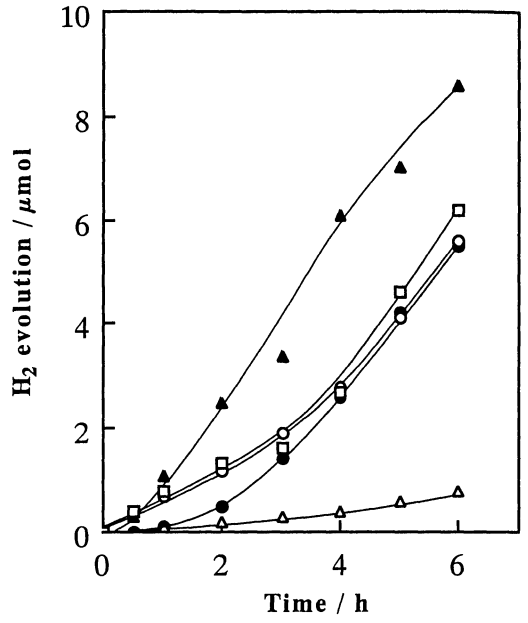

Fig. 7. Water-photoreductive H_2 evolution catalyzed by F-OPP-*n* and OPP-*n* in the presence of $RuCl_3$: (●) F-OPP-3; (▲) F-OPP-4; (○) OPP-3; (△) OPP-4; (□) FH-OPP-3 (in the presence of $RhCl_3$).

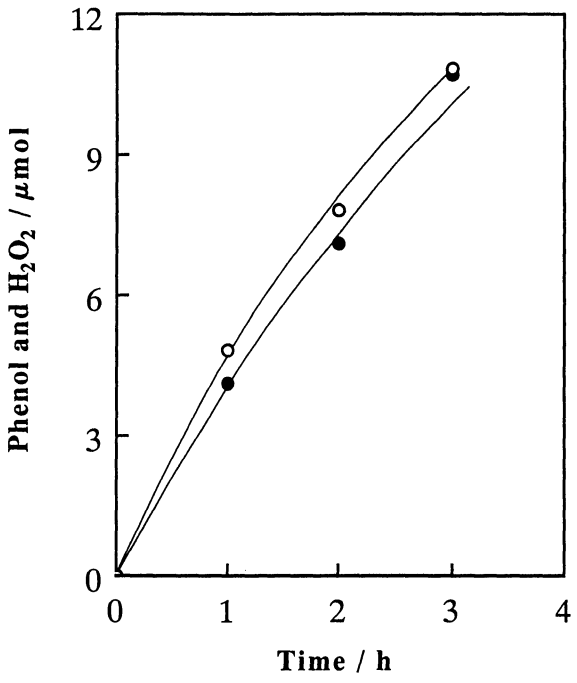

Fig. 8. F-OPP-3-catalyzed photooxidation of benzene in O_2-saturated aqueous acetonitrile: (●) phenol; (○) H_2O_2.

Table 3. Comparison of Catalysis of F-OPP-*n* and OPP-*n* on Photolysis of TEA in the Presence of $RuCl_3$

Catalyst	Photoproducts[a]/μmol		
	H_2	DEA	EtOH
F-OPP-2	1.1	—	—
F-OPP-3	5.5	24.5	5.3
F-OPF-4	8.6	17.3	4.0
OPP-2	0.8	—	—
OPP-3	5.6	42.0	29.0
OPP-4	0.8	14.0	1.2

a) After irradiation at λ>290 nm for 6 h.

was the case with OPP-2. A careful examination of the F-OPP-3 system revealed that F-OPP-3 should undergo defluorination, leading to the consumption of F-OPP-3, even in the presence of Ru^0. In fact, compared with the total reduction products of H_2 and ethanol, DEA as the oxidation product was produced in a larger amount. This fact is consistent with the photoreductive defluorination of F-OPP-3 during photocatalysis. From the photocatalytic reaction using F-OPP-3, the formation of FH_2-OPP-3 was also confirmed to be a defluorinated product. Interestingly, FH_2-OPP-3 showed photocatalytic activity under comparable conditions, as is shown in Fig. 7. It is now clear that the degradation of F-OPP-*n* is unavoidable, even during the Ru^0-mediated H_2 evolution, and that the partially defluorinated FH_2-OPP-3 still has photocatalytic activity.

F-OPP-3-Catalyzed Photooxidation of Benzene with O_2.[14] It was noticed that F-OPP-3 should be difficult to oxidize because of the high oxidation potential; it was stable under UV irradiation in acetonitrile in the presence of O_2. Taking these facts into account, an F-OPP-3-catalyzed photooxidation of benzene with O_2 was attempted in acetonitrile under λ>290 nm irradiation. The acetonitrile solution of F-OPP-3 (1.0×10^{-3} mol dm^{-3}) containing benzene (20 vol%) and H_2O (2 vol%) was saturated with O_2, and was irradiated with λ>290 nm light. As shown in Fig. 8, almost equal quantities of phenol and hydrogen peroxide (H_2O_2) were increasingly formed. Oxygen was confirmed to be essential for the photoformation of phenol. In addition, the consumption of F-OPP-3 was found to be negligible during photooxidation. The formation of phenol was never observed when F-OPP-3 was removed or replaced by OPP-3. However, small quantities of H_2O_2 were detected in both cases after 3 hours of irradiation; in the former case, 0.4—0.7 μmol, and in the latter case, 1.5—1.8 μmol. When F-OPP-4 was employed instead of F-OPP-3, the formation of phenol and H_2O_2 was almost doubled under the same conditions.

Figure 9 depicts typical results of the F-OPP-3-catalyzed photooxidation of benzene under O_2 with varying concentrations of water. Trace amounts of phenol and H_2O_2 were produced, even without the addition of water, which is probably attributable to the presence of moisture in the system; their production increased with increasing the concentration of water up to 2—3 vol%.

Semiempirical Molecular Orbital Calculation of Anion and Cation Radicals Derived from OPP-3 and F-OPP-3. In a previous paper concerning the photoca-

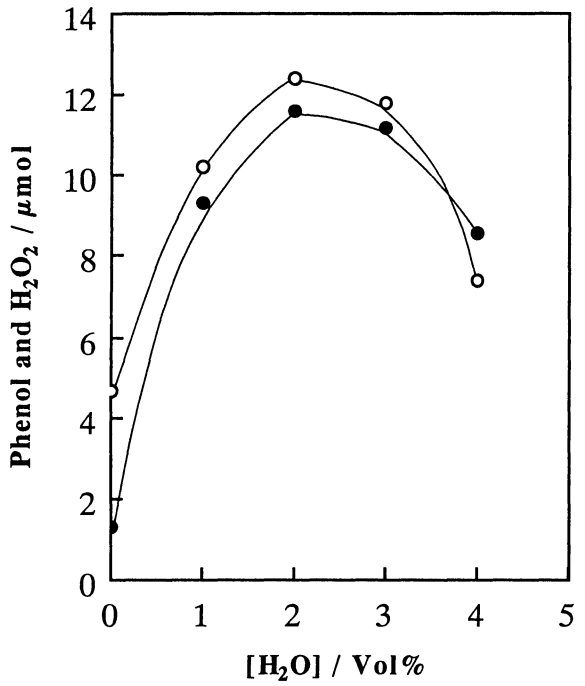

Fig. 9. Effect of the addition of water on the formation of phenol (●) and H_2O_2 (○) in O_2-saturated acetonitrile after irradiation for 3 h.

talysis of OPP-*n*, intermediary OPP-*n*$^{-\cdot}$ was speculated to have a coplanar quinonoid-like structure on the basis of the transient spectra of OPP-*n*$^{-\cdot}$.[7b,c,15] The molecular orbital (MO) calculation using the MOPAC system (the MNDO/PM3 method)[16] revealed that, as shown in Fig. 10b, OPP-3$^{-\cdot}$ has an almost coplanar configuration, while OPP-3, itself, has a twisted configuration (Fig. 10a). The bond length between the phenylene rings and those of the other C–C bonds in the phenylene rings parallel to C1–C1′ and C1″–C4′ bonds are slightly shortened in OPP-3$^{-\cdot}$, compared with those of OPP-3, thus supporting the quinonoid-like structure. The computer-optimized structure of OPP-3$^{-\cdot}$ is quite consistent with a large bathochromic shift in the transient spectrum of OPP-3$^{-\cdot}$, due to conjugation through the molecules.[7b,c,15]

With these facts in view, the MOPAC MO calculation (MNDO/PM3) was extended to the F-OPP-2 and F-OPP-3 systems.[16] The results are summarized in Table 4 along with those for the OPP-2 and OPP-3 systems.

The computer-optimized structures of OPP-2, OPP-3, F-OPP-2, and F-OPP-3 should reflect their vapor-phase structures, and are in fairly good agreement with the structures determined experimentally in the vapor phase or in solution, rather than those based on crystallographic analysis.[3b,17]

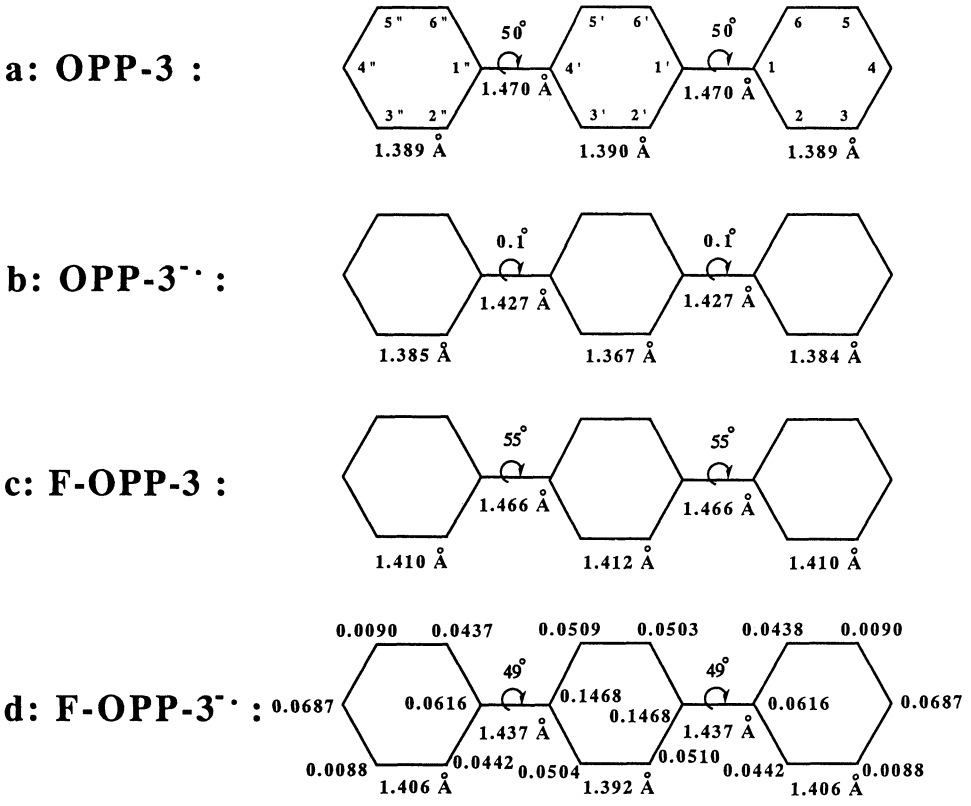

Fig. 10. Structures and spin densities of OPP-3, OPP-3$^{-\cdot}$, F-OPP-3, and F-OPP-3$^{-\cdot}$ calculated by using the MNDO/PM3 method. The C–C bond lengths and the torsion angles of the benzene rings are shown in Å and deg, respectively. For F-OPP-3$^{-\cdot}$, the spin densities on the carbon atoms are shown at each carbon atom.

Table 4. Computer-Assisted Calculation of Anion Radicals and Cation Radicals of F-OPP-3, F-OPP-2, OPP-3, and OPP-2

	Dihedral angles/degree		C–F bond length/Å		IP/eV	
	Calculated	Experimental	C4–F	C2′–F	Calculated	Experimental[a]
OPP-2	50	45±10[b]	—	—	9.16 (8.70)[a]	8.32
OPP-3	50	—	—	—	8.93 (8.43)[a]	8.20
F-OPP-2	55	70[c]	1.334	—	10.64	
F-OPP-3	55	—	1.334	1.338	10.57	
OPP-2$^{-\cdot}$	0.1	—	—	—		
OPP-3$^{-\cdot}$	0.1	—	—	—		
F-OPP-2$^{-\cdot}$	45	—	1.339	—		
F-OPP-3$^{-\cdot}$	49	—	1.339	1.344		
OPP-2$^{+\cdot}$	0.1	—	—	—		
OPP-3$^{+\cdot}$	0.8	—	—	—		
F-OPP-2$^{+\cdot}$	45	—	1.320	—		
F-OPP-3$^{+\cdot}$	48	—	1.324	1.332		

a) See Ref. 20. b) See Ref. 17a. c) See Ref. 17b.

Table 5. Differences between the Heat of Formation for Neutral Molecules and Anion Radicals

	ΔH/kcal mol^{-1} [a]
OPP-2	−17.1
OPP-3	−26.0
OPP-4	−30.2
F-OPP-2	−55.4
F-OPP-3	−60.5

a) $\Delta H = H$(anion radical) − H(neutral molecule). These values were obtained from MO calculation using MOPAC system (MNDO/PM3).[16]

Both of the dihedral angles between the phenylene rings in the optimized structures of F-OPP-2 and F-OPP-3 are about 55°, thus being larger than their nonperfluorinated species, OPP-2 and OPP-3, as exemplified by F-OPP-3 in Fig. 10c. For the anion radicals, the dihedral angles are 45° and 49°, respectively, while that of the nonfluorinated species is almost 0° (Fig. 10b). The lengths of the bond between the phenylene rings (C1–C1′ bond) in the anion radicals of F-OPP-2 and F-OPP-3 are shorter than those in the neutral molecules. In addition, the C–C bonds in the phenylene rings parallel to the C1–C1′ bond (C2–C3, C5–C6, C2′–C3′, and C5′–C6′ bonds in F-OPP-2$^{-\cdot}$, and C2–C3, C5–C6, C2′–C3′, C5′–C6′, C2″–C3″, and C5″–C6″ bonds in F-OPP-3$^{-\cdot}$) are also slightly shortened in the anion radicals, compared with the respective F-OPP-2 and F-OPP-3, as exemplified by F-OPP-3 in Fig. 10d. These facts imply that the anion radicals might partially take a quinonoid-like structure, in spite of their noncoplanar structure.

Interestingly, as shown in Table 5, the differences between the heats of formation for neutral molecules and anion radicals, which were calculated by MOPAC MO calculations (MNDO/PM3), are more negative for the F-OPP-*n* series, compared with the nonfluorinated OPP-*n* series, implying ease of their anion radical formation.

The lengths of the C–F bonds are slightly longer for the anion radical than for the neutral molecule, suggesting that the bond strength of the C–F bonds are weakened in the anion radical. An evaluation of the bond strengths of each C–F bond ensured the weakening of all C–F bonds in the anion radical, compared to the neutral molecule.[18] This implies that the C–F bond at the 4 and 4″ positions are more weakened than the others. It is interesting to note that higher spin densities were found on the carbons at the positions of C1(0.0616), C1′(0.1468), C1″(0.0616), C4(0.0687), C4′(0.1468), and C4″(0.0687). Since it is expected that the elimination of F^- from F-OPP-3$^{-\cdot}$ is caused most readily at a high spin-density position, these calculation results are consistent with the practical positions of the defluorination from F-OPP-3.

On the other hand, the MOPAC MO calculations show that the C–F bonds are stabilized more in F-OPP-3$^{+\cdot}$ than in the neutral molecule, F-OPP-3. This is demonstrated by both a shortening of the C–F bonds (the average decrease of the C–F bond lengths is 0.009 Å, compared to that of the neutral molecule), and the energetic stabilization of the C–F bonds shown in the evaluation with the MOPAC system.[18] This stabilization of the cation radical explains the stability of F-OPP-3 during photooxidation of benzene in the presence of O_2 where the cation radical is considered to be involved in the reaction mechanism. A similar tendency regarding stabilization was also observed for F-OPP-2$^{+\cdot}$, as shown in Table 4.

The calculated ionization potentials (IP) of nonfluorinated OPP-*n* and perfluorinated ones (F-OPP-*n*) indicate that it should be more difficult to oxidize F-OPP-2 and F-OPP-3 than OPP-2 and OPP-3, respectively (Table 4). This fact suggests the difficulty regarding the oxidation of F-OPP-3; once F-OPP-3$^{+\cdot}$ is formed oxidatively, it should show a high oxidation ability, being consistent with the photooxidative catalysis of F-OPP-3.

Mechanism of Photocatalysis of F-OPP-3. Since

the onset in the absorption spectrum of F-OPP-3 under the above-mentioned reaction conditions is at around λ=310 nm, irradiation with a high-pressure mercury lamp through a Pyrex tube leads to photoexcitation by λ=297 and λ=303 nm light of the lamp. As dissipation mechanisms of the initial singlet F-OPP-3 (^{1}F-OPP-3*) in an organic solvent, an excimer (F-OPP-3)$_2$* through triplet F-OPP-3 (^{3}F-OPP-3*) should be formed, accompanied by an immediate charge transfer in a solvent cage, as depicted in Scheme 2. The photodefluorination of F-OPP-3 is explained as being due to the formation of F-OPP-3$^{-\cdot}$ from the excimer (F-OPP-3)$_2$* (Eq. 2). The photodefluorination under λ=366 nm irradiation in the presence of benzophenone suggests the participation of ^{3}F-OPP-3*, i.e., a triplet energy transfer from excited benzophenone to F-OPP-3 during photodefluorination. The formation of F-OPP-3$^{+\cdot}$ was supported by the identification of methoxylated F-OPP-3 regarding photolysis in methanol (Eq. 3).

When a good electron donor, TEA, is present in the photolysate, the photodefluorination of F-OPP-3 should proceed solely through an exciplex, followed by the formation of F-OPP-3$^{-\cdot}$, as depicted by Eq. 4 in Scheme 2. As a photodefluorination product, FH$_2$-OPP-3 was practically isolated (Eq. 5). These observations are in agreement with a computer-assisted calculation of the structure of F-OPP-3$^{-\cdot}$, showing a weakening of the C–F bonds of F-OPP-3$^{-\cdot}$, and spin localization at the terminal carbon atoms.

When a colloidal noble metal, such as Ru^0 or Rh^0, is present in the photoreaction system, it mediates an electron transfer from F-OPP-3$^{-\cdot}$ to water, leading to the reduction of water to H_2 evolution (Eq. 6).

Oxygen is well-known to work as a triplet quencher; it then suppresses the photodefluorination of F-OPP-3 in the solvent. On the other hand, when O_2 is present as a good electron acceptor in the photocatalytic system, ^{1}F-OPP-3* might be expected to be oxidatively quenched, giving both F-OPP-3$^{+\cdot}$ and $O_2^{-\cdot}$ (Eq. 7). The F-OPP-3-catalyzed photooxidation of benzene in the presence of water can be explained to proceed through the oxidation of OH$^-$ by F-OPP-3$^{+\cdot}$ (Eq. 9) and a reaction of the

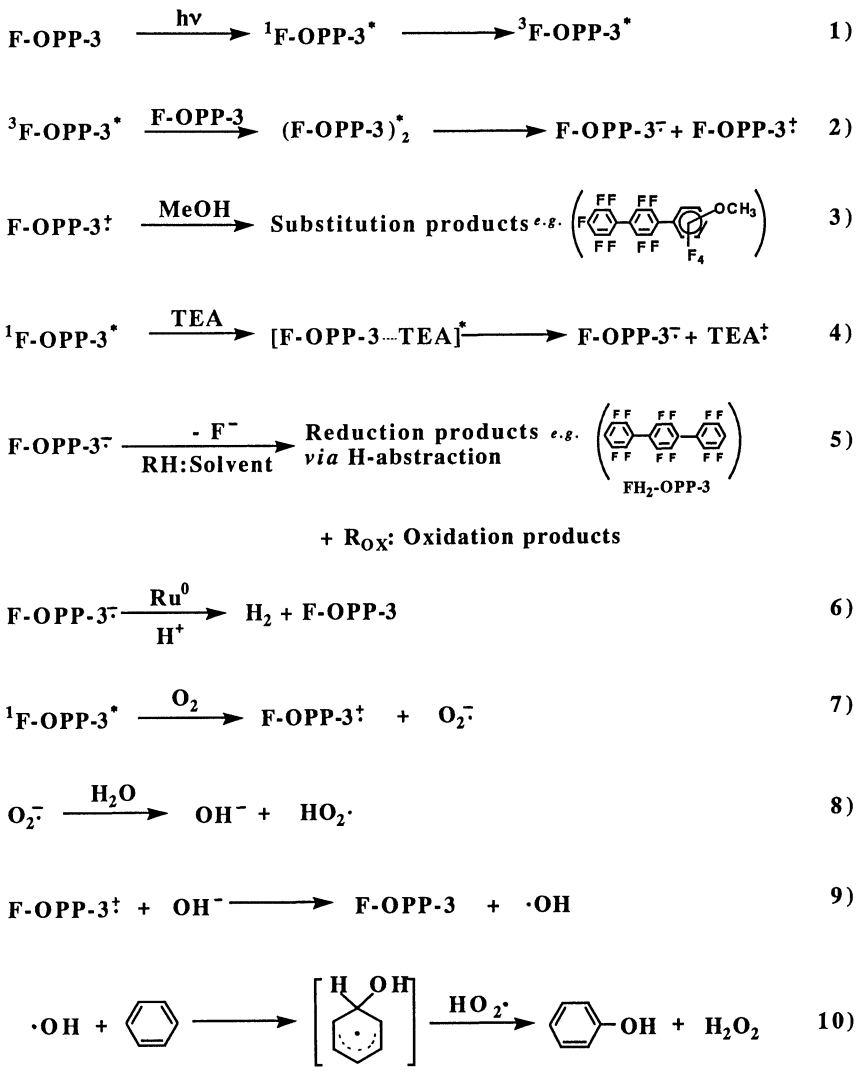

Scheme 2.

OH radical with benzene (Eq. 10). The oxidation potential of OH^- to $OH^\cdot$ is 0.56 V vs. SCE (in acetonitrile) and 1.66 V vs. SCE (in H_2O);[19] F-OPP-3$^{+\cdot}$ is then essentially able to oxidize OH^- to $OH^\cdot$. The spectral detection of the formation of F-OPP-3$^{+\cdot}$ was found to be impossible, since F-OPP-3 shows emission over a wide wavelength region from UV to visible, which overlaps with the anticipated absorption of the radical cation. However, the MO calculation has shown that the C–F bonds are stabilized more in F-OPP-3$^{+\cdot}$ than in the neutral molecule, F-OPP-3, due to a shortening of the C–F bonds (Table 4).

The proposed mechanism for the oxidation of benzene is quite comparable with that of the TiO_2–catalyzed photooxidations of aromatic hydrocarbons. Photoexcited TiO_2 undergoes oxidative quenching by O_2 without any electron mediator, giving $O_2^{-\cdot}$. The hole on the quenched TiO_2 oxidizes water or organic substrates in the system, leading to the oxidation of aromatic hydrocarbons.

Conclusion

Perfluorination of OPP-*n* induces various changes in the physical and spectral characteristics of OPP-*n*; those are mainly caused by a steric repulsion between the fluorine atoms on neighboring rings. F-OPP-*n*, itself, undergoes defluorination through F-OPP-$n^{-\cdot}$ formed upon UV irradiation in a solvent. When a redox couple which can remove an electron from F-OPP-$n^{-\cdot}$ is present in the photoreaction system, however, the degradation of F-OPP-*n* is inhibited and F-OPP-*n*, itself, is able to work as a photocatalyst in the presence of such an electron donor and electron acceptor. F-OPP-3 shows efficient photocatalytic activity for the reduction of water to H_2 upon irradiation of heterogeneous suspensions in an aqueous organic solution in the presence of triethylamine as an electron donor and Ru^0 colloid as an electron relay between F-OPP-$3^{-\cdot}$ and water. In the presence of O_2, the photoexcited F-OPP-3 is quenched; resulting F-OPP-3$^{+\cdot}$ leads to the oxidation of water and benzene to H_2O_2 and phenol, respectively. The important and fundamental concept that we obtained in this study is how to combine in one system both the reductive and oxidative aspects of the photocatalyst with logical and practical redox couples as reactants, which is essential for any practical applications of photocatalytic systems.

Experimental

Materials. Bromopentafluorobenzene and decafluorobiphenyl were obtained from Aldrich Chemical Company and biphenyl (OPP-2), *p*-terphenyl (OPP-3), and *p*-quaterphenyl (OPP-4) (guaranteed (GR) grade from Nacalai Tesque) were used without further purification. $RhCl_3$ and $RuCl_3 \cdot nH_2O$ (extra-pure (EP) grade) and $H_2PtCl_6 \cdot nH_2O$ (GR grade) were obtained from Nacalai Tesque, and $PdCl_2$ (GR grade) from Kishida Chemicals. The titanium sulfate solution used for the analysis of H_2O_2 was obtained from Nacalai Tesque. For cyclic-voltammetry, acetonitrile was dried over 4A-16ϕ molecular sieves and distilled before use. Tetrabutylammonium hexafluoro phosphate ($TBAPF_6$), which was obtained from Tokyo Kasei as GR grade, was recrystallized from ethanol/water (1 : 1), and dried under vacuum before use. The other chemicals used in this study were identical to those used in previous studies.[7]

Analysis. The formation of H_2 was analyzed by GLC on an activated carbon column (2 m×3 mm) of a Shimadzu Model GC-12A at 100 °C. A product analysis was carried out by GLC on a Shimadzu Model GC-7AF and GC-12A apparatus equipped with a flame ionization detector and the following columns: a 3 m×3 mm ASC-L column for diethylamine, ethanol and acetaldehyde; a 1 m×3 mm PEG 20 M column for phenol and F-OPP-3; a 25 m×0.2 mm Shimadzu capillary column of OV-1 for F-OPP-3 and defluorination product of F-OPP-3 itself (carrier gas N_2; carrier gas pressure 0.4 kg cm^{-2}; column temperature 240 °C; injector temperature 250 °C).

GC mass analysis was conducted on JEOL Model JMS-DX with a 25 m×0.2 mm capillary column of OV-1 for the analysis of products from photolysate of F-OPP-3 in methanol.

UV-vis spectra were recorded on a Hitachi Model 220A spectrophotometer. Steady-state photoluminescence spectra were recorded on a Hitachi Model 850 spectrofluorometer. The lifetime of the photoluminescence was measured using a Horiba NASE-1100.

The fluorescence quantum yield was determined by using biphenyl and 4-trifluoromethyl-*p*-terphenyl[3c] as standard reagents.

The oxidation potential of F-OPP-3 was determined by cyclic voltammetry in dried acetonitrile. An acetonitrile solution containing 2.0×10^{-4} mol dm^{-3} of F-OPP-3 and 0.1 mol dm^{-3} of tetrabutylammonium hexafluorophosphate ($TBAPF_6$) was prepared, deaerated by argon gas, and subjected to measurement. A platinum wire and a plate were used as the working electrode and counter electrode, respectively. The reference electrode used was a saturated calomel electrode (SCE).

The ^{19}F NMR data were obtained on a JEOL JNM-PAX-100 or Burker AM-600. ^{19}F NMR chemical shifts are reported in ppm relative to external 4-fluorotoluene on the δ scale. The ^{1}H NMR data were obtained on a JEOL JNM-GSX-400 spectrometer. The ^{1}H NMR spectra are reported in ppm from internal standard tetramethylsilane (TMS) on the δ scale. The mass spectral data were obtained on a JEOL JMS-DX303 spectrometer. The infrared spectral data were obtained on a Hitachi Model 260-10 or a JEOL-AQS20M spectrometer.

Synthesis of F-OPP-3 and F-OPP-4.[2] Bromopentafluorobenzene (4.96 g, 2.0×10^{-2} mol) in dry THF (10 ml) was added to magnesium turnings (0.54 g, 2.2×10^{-2} mol) in dry THF (10 ml) stirred under mild heating. To the resulting Grignard solution was added decafluorobiphenyl (10.17 g, 3.0×10^{-2} mol) dissolved in dry THF (10 ml) under ice-cooling. The resulting solution was stirred at room temperature in order to allow the Grignard reagent to react with decafluorobiphenyl. After completion of the reaction (color change to white), the reaction mixture was poured into a dilute HCl methanolic solution (100 ml) under ice-cooling, and stirred at room temperature overnight. The white precipitate (11.34 g) was collected by filtration and thoroughly washed with water, then

dried in vacuo. After a mixture of F-OPP-3 and F-OPP-4 was roughly purified by Soxhlet extraction using methanol as the extractant, F-OPP-3 and F-OPP-4 was separated by column chromatography using silica-gel column and cyclohexane as the eluate.

F-OPP-3; IR (KBr) 1660, 1540, 1500, 1470, 1270, 1180, 1100, 1000, 960, 940, 710 cm^{-1}. ^{19}F NMR (100 MHz, $CDCl_3$) δ=−45.13 (t, 4F), −33.47 (t, 2F), −19.65 (s, 8F). MS, *m/z* 482 (M^+). Found: C, 44.54; F, 54.36%. Calcd for $C_{18}F_{14}$: C, 44.81; F, 55.19%.

F-OPP-4; IR (KBr) 1660, 1530, 1500, 1460, 1260, 1180, 1000, 960, 710 cm^{-1}. ^{19}F NMR (100 MHz, $CDCl_3$) δ=−45.35 (br, 4F), −33.26 (br, 2F), −19.44 (d, 12F). MS, *m/z* 630 (M^+). Found: C, 45.41; F, 53.48%. Calcd for $C_{24}F_{18}$: C, 45.71; F, 54.28%.

Preparation of FH_2-OPP-3. FH_2-OPP-3 was obtained from the reaction mixture of an F-OPP-3-catalyzed photoreduction of water to H_2 and the photolysis of F-OPP-3 in methanol. It was purified by column chromatography using silica-gel column and cyclohexane as the eluate.

FH_2-OPP-3; IR (KBr) 3080, 1610, 1500, 1470, 1440, 1380, 1270, 1230, 1180, 1120, 1060, 1000, 930, 860, 800, 740, 700 cm^{-1}. ^{19}F NMR (600 MHz, $CDCl_3$) δ=−73.44 (br, 4F), −72.62 (t, 4F), −72.44 (s, 4F). The ^{19}F NMR chemical shifts are reported in ppm relative to external (trifluoromethyl)benzene on the δ scale. ^1H NMR (400 MHz, ^8d-THF) δ=7.83 (m, 2H). MS, *m/z* 446 (M^+).

Preparation of Ru Colloid.[13] Ru colloid was prepared by the reduction of $RuCl_3$ with citrate as the reducing agent: A 0.1 % sodium citrate solution (100 ml) containing $RuCl_3$ (16 mg) was kept at 100 °C overnight. The resulting colloid suspensions were centrifuged and dialyzed.

Procedure for Photolysis of F-OPP-3. Each solution of F-OPP-3 (1.0×10^{-3} mol dm^{-3}, 2 ml) was placed in a Pyrex tube (8 mm in diameter). After those homogeneous solutions were purged with argon gas, the tubes were closed off with a gum stopper and then irradiated at λ>290 nm by using a 500 W high-pressure mercury arc lamp. For the sensitized photolysis of F-OPP-3, a mixture of F-OPP-3 (1.0×10^{-3} mol dm^{-3}) and benzophenone (0.1 mol dm^{-3}) in THF (2 ml) was irradiated under λ=366 nm light. The photolysis in the presence of O_2 was carried out after the introduction of O_2 to a THF solution (2 ml) of F-OPP-3 (1.0×10^{-2} mol dm^{-3}). The product analysis was performed by GLC (capillary column of OV-1) and GC-MS analysis.

Determination of Quantum Yield of Photolysis of F-OPP-3. Quantum yields were determined by using a potassium tris(oxalato)ferrate(III) actinometer over a concentration range of 0.0002—0.001 mol dm^{-3} of a F-OPP-3 solution. The incident light (λ=302 nm) was isolated from a xenon lamp (500 W) using a WACOM XD-501S monochrometer.

Photoreduction of H_2O to H_2. As reported in a previous paper,[7] F-OPP-*n* (10 mg *n*=2,3,4) was added to a mixture of water (0.5 ml, 2.78×10^{-2} mol), triethylamine (0.5 ml, 3.58×10^{-3} mol), and methanolic $RuCl_3$ solution (0.5 ml, 6.0×10^{-3} mol dm^{-3}) in a Pyrex tube (8 mm in diameter). The resulting suspension was flashed with argon gas under ice-cooling, closed off with a gum stopper, and then irradiated under magnetic stirring at λ>290 nm by using a 500 W high-pressure mercury arc lamp. The gaseous and liquid products were analyzed by GLC, as reported previously.[7]

Photooxidation of Benzene with F-OPP-3. An acetonitrile solution of F-OPP-3 (1.0×10^{-3} mol dm^{-3}, 2 ml) containing benzene (20 vol%) and a small quantity of H_2O (0—4 vol%) was irradiated at λ>290 nm from a 500 W high-pressure mercury arc lamp for 3 h; the resulting photolysate was analyzed by GLC. The formation of hydrogen peroxide was analyzed by a colorimetry method by monitoring the absorbance at λ=402 nm due to the absorption of a complex of H_2O_2 with $Ti(SO_4)_2$.

The authors thank Sony Tektronix Corporation for the MOPAC calculations with the CAChe system. This research was supported by a grant-in-aid for Scientific Research No. 03203119 from the Ministry of Education, Science and Culture. The research was also conducted as a theme of the Research Society for CO_2-Fixation sponsored by the Institute of Laser Technology under the commission of The Kansai Electric Power Company, Inc. The financial aid provided by RITE and the Shorai Foundation for Science and Technology is also gratefully acknowledged.

References

1) a) G. Camaggi and F. Gozzo, *J. Chem. Soc. C,* **1969**, 489; b) I. Haller, *J. Am. Chem. Soc.,* **88**, 2070 (1966).

2) a) J. L. Cotter, G. J. Knight, J. M. Lancaster, and W. W. Wright, *J. Appl. Polym. Sci.,* **12**, 2481 (1968); b) G. M. Brooke, R. D. Chambers, J. Heyes, and W. K. R. Musgrave, *J. Chem. Soc.,* **1964**, 729.

3) a) A. J. Bilbo and G. M. Wyman, *J. Am. Chem. Soc.,* **75**, 5312 (1953); b) D. E. Fenton, *Chem. Ind. (London),* **24**, 695 (1969); c) W. Zapka and U. Brackmann, *Appl. Phys.,* **20**, 283 (1979).

4) C. R. Brundle, M. B. Robin, and N. A. Kuebler, *J. Am. Chem. Soc.,* **94**, 1466 (1972).

5) J. F. Liebman, A. Greenberg, and W. R. Doliver, Jr., "Molecular Structure and Energetic," VCH Publishers, Inc., 1988, Vol. 8, pp. 19—41.

6) a) P. K. Freeman and R. Srinivasa, *J. Org. Chem.,* **52**, 252 (1987); b) P. K. Freeman and N. Ramnath, *J. Org. Chem.,* **56**, 3646 (1991).

7) a) S. Matsuoka, H. Fujii, C. Pac, and S. Yanagida, *Chem. Lett.,* **1990**, 1501; b) S. Matsuoka, H. Fujii, T. Yamada, C. Pac, A. Ishida, S. Takamuku, M. Kusaba, N. Nakashima, S. Yanagida, K. Hashimoto, and T. Sakata, *J. Phys. Chem.,* **95**, 5802 (1991); c) S. Matsuoka, T. Kohzuki, C. Pac, A. Ishida, S. Takamuku, M. Kusaba, N. Nakashima, and S. Yanagida, *J. Phys. Chem.,* in press.

8) S. Matsuoka, T. Kohzuki, A. Nakamura, C. Pac, and S. Yanagida, *J. Chem. Soc., Chem. Commun.,* **1991**, 580.

9) a) R. O. Loutfy, *Can. J. Chem.,* **54**, 1454 (1976); b) K. Meerholz and J. Heinze, *J. Am. Chem. Soc.,* **111**, 2325 (1989); c) K. Meerholz and J. Heinze, *Angew. Chem., Int. Ed. Engl.,* **29**, 692 (1990).

10) A. J. Bard and H. Lund, "Encyclopedia of Electrochemistry of the Elements," Marcel Dekker, Inc., New York (1978), Vol. XV.

11) B. Chittim, S. Safe, N. J. Bunce, L. O. Ruzo, K. Olie, and O. Hutzinger, *Can. J. Chem.,* **56**, 1253 (1978).

12) a) P. K. Freeman, N. Ramnath, and A. D. Richardson, *J. Org. Chem.,* **56**, 3643 (1991); b) J. P. Soumillion and B. D. Wolf, *J. Chem. Soc., Chem. Commun.,* **1981**, 436.

13) I. Willner, R. Maidan, D. Mandler, H. Durr, G. Dorr,

and K. Zengerle, *J. Am. Chem. Soc.*, **109**, 6080 (1987).
14) a) M. Fujihira, Y. Satoh, and T. Osa, *Nature*, **293**, 206 (1981); b) Y. Shimamura, H. Misawa, T. Oguchi, T. Kanno, H. Sakuragi, and K. Tokumaru, *Chem. Lett.*, **1983**, 1691.
15) T. Shida, *J. Phys. Chem.*, **82**, 991 (1978).
16) The calculations for OPP-2, OPP-3, and F-OPP-2, were carried out by MOPAC Ver. 5.0 (QCPE No. 445), J. J. P. Stewart, "QCPE Bull. 1989, 9, 10,"; Tsuneo Hirano, "JCPE Newsletter, 1989," 1 (2), 36; Revised as Ver. 5.01 by Jiro Toyoda, for OS/2 Personal Computers (NEC PC-9801), "JCPE Newsletter, 1990," 2 (1) 56; and those for F-OPP-3 were done by MOPAC Ver. 5.10 or 6.10 using CAChe system.
17) a) O. Bastiansen, *Acta Chem. Scand.*, **3**, 408 (1949); b) A. Almenningen, A. O. Hartmann, and A. M. Seip, *Acta Chem. Scand.*, **22**, 1013 (1968); c) H. Cailleau, J. L. Baudour, and C. M. E. Zeyen., *Acta Crystallogr., Sect. B*, **35**, 426 (1979); d) J. L. Baudour, Y. Delugeard, and H. Cailleau, *Acta Crystallorg., Sect. B*, **32**, 150 (1976).
18) The strengths of the C–F bonds were evaluated by the values of the total electronic and nuclear energies obtained by using the key word, ENPART. The average decrease in the value for the cation radical was 0.29 eV compared to that of the neutral molecule.
19) L. Eberson, *Acta Chem. Scand., Ser. B*, **38**, 439 (1984).
20) J. L. Bredas, R. Silbey, D. S. Boudreaux, and R. R. Chance, *J. Am. Chem. Soc.*, **105**, 6555 (1983).